THE NUCLEUS OF COMET HALE–BOPP (C/1995 O1): SIZE AND ACTIVITY

YANGA R. FERNÁNDEZ
University of Hawaii, Institute for Astronomy, 2680 Woodlawn Drive, Honolulu, HI 96822, USA
E-mail: yan@ifa.hawaii.edu

(Received 15 March 2002; Accepted 22 June 2002)

Abstract. A review of our current understanding of Comet Hale–Bopp's nuclear size is presented. Currently the best constraints on the effective radius are derived from late-1996 mid-IR data and near-perihelion radio data. Unfortunately the two regimes give differing answers for the radius. A possible reconciliation of the two datasets is presented that would place the radius at around 30 km. This is a large cometary radius compared to the others that are known, and this motivates a discussion of what makes a large comet different. From several possible large-comet properties, Hale–Bopp's activity is analyzed, focusing on the production rates, coma jet features, dust optical depth, and relationship with the interplanetary dust environment. The optical depth is particularly important since an optically-thick inner coma could complicate attempted measurements of the "nucleus".

Keywords: Comets, Hale–Bopp

1. Introduction

Comet Hale–Bopp, C/1995 O1, provided one of the most spectacular apparitions of the late 20th Century. The source of this striking event was the nucleus within the comet's head, and various methods were used by many workers to reveal the physical and compositional nature of this icy conglomerate. This is a broad topic so only the question of the nucleus's size (in the form of the effective radius) will be addressed in Section 2. While the current answer is not yet definitive, it is nonetheless clear that the nucleus is one of the largest ever to have been measured, and this motivates the question: "How is a big comet different?" There are many properties that one might use to answer this, but, again, with such a broad topic, the discussion in Section 3 will be restricted to the comet's prodigious dust activity. The production of large quantities of dust grains effected several unusual situations that rarely, if ever, have been seen in comets before.

This review will build upon previously-published discussions of Hale–Bopp's size and activity. Most importantly, the size of the nucleus is discussed in a review by Weaver and Lamy (1997), and the activity, as it related to the comet's visual countenance, is discussed in a review by Kidger (1997).

Earth, Moon and Planets **89:** 3–25, 2002.

2. Size

2.1. Background

Historically it has been difficult to know when one was observing the nucleus and not just being fooled by a surrounding inner coma. Certainly many observations of comets taken at relatively small heliocentric distance r are only sensitive to the coma. At larger r, where one expects the comet to be inactive, not only can one still be misled by a low level of activity, but also many nuclei are infeasibly faint. Jewitt (1991) summarized the minimum criteria for determining if one were observing a bare nucleus, and unfortunately not one of these criteria has yet been satisfied in any visible- or infrared-wavelength observation of Hale–Bopp, even now with the comet at $r > 15$ AU. Our understanding of Hale–Bopp's size has come from processing these short-wavelength observations to indirectly extract the nucleus and from long-wavelength (radio) information where the interfering coma is not as strong. In this section the various methods used to probe Hale–Bopp's nucleus will be discussed, along with a few methods that are not yet applicable to this comet. Generally the methods to determine the effective radius R can be divided into those that do require knowing the thermal behavior of the nucleus, and those that do not.

2.1.1. *Methods Incorporating Thermal Behavior*

The measured gas production rate can be used to derive a minimum value for R, assuming that all of the gas coma sublimates from a nuclear (as opposed to an extended, comatic) source. One uses the known vaporization rate of water ice at a given temperature (derived from the comet's r) to calculate the minimum area needed to provide the observed gas flux. This vaporization rate is given by, e.g., Cowan and A'Hearn (1979), and it depends on the nucleus's albedo, though only weakly for low-albedo objects. From measurements of the gas emitted by Hale–Bopp near perihelion, Schleicher et al. (1997) found $R \geq 8.5$ km, and Weaver et al. (1999) found $R \gtrsim 10$ km. There is evidence for a diffuse source of some cometary parent molecules (e.g., DiSanti et al., 1999) but apparently nearly all of the water comes directly from the nucleus (Dello Russo et al., 2000), so the lower limit to R is likely to be robust with respect to that issue. However Harris, W. M., Morgenthaler, J. P., Scherb, E., Anderson, C., and Oliversen, R. J.: 2002 (these proceedings) have noted that Hale–Bopp's intense activity could complicate the usual Haser-model conversion from gas-coma brightness to production rate, and so this could indirectly affect the lower limits on R.

A very popular method that the comet community has borrowed from the asteroid community is to use radiometry. The thermal continuum is measured and simultaneous visible-wavelength observations are used to constrain R and the geometric albedo p. The method was first performed about 30 years ago (Allen, 1970; Matson, 1972; Morrison, 1973), and is described in detail by Lebofsky and Spencer (1989). The critical step is to calculate a surface temperature map using a thermal

model, and there are two simple, widely-used models, covering the extremes of thermal behavior. One, for slow-rotators ("standard thermal model"), applies if the rotation is so slow (or the thermal inertia so low) that every point on the surface is in instantaneous equilibrium with the impinging solar radiation. The other, for fast-rotators ("isothermal latitude model"), applies if the rotation is so fast (or the thermal inertia so high) that a surface element does not appreciably cool as it spins away from local noon and out of sunlight. This model also assumes that the rotation axis is perpendicular to the Sun–Earth-object plane. For an axis that points at the Sun, the two models predict the same temperature map. Of the nuclei that have been studied, nearly all appear to be slow-rotators. The only apparent exception so far is 107P/Wilson–Harrington (Campins et al., 1995).

The complexity of the thermal models can be greatly expanded, and there exist several such models that account for the thermal properties of the nucleus's bulk material in order to sample the middle ground between the two thermal extrema just described. Unfortunately most of the critical thermal quantities are as yet very unconstrained. A paper by Prialnik, D.: 2002 (these proceedings) discusses the current state-of-the-art in nucleus thermal modeling.

Unfortunately we are as yet unable to apply the simple thermal models directly to Hale–Bopp data – the comet has yet to be seen in an inactive state, so observations of the nucleus are contaminated by coma. At time of writing, $r > 15$ AU, and Hale–Bopp still possesses a dust coma; in comparison, 1P/Halley was apparently inactive at $r = 18.8$ AU (Hainaut et al., 1995). If Hale–Bopp becomes inactive by 2008 (corresponding to $r \leq 27$), then it will be possible to use the MIPS instrument on the SIRTF spacecraft to obtain radiometric measurements of the nucleus. In MIPS's 24 and 70 μm bands the comet will emit a few millijanskys and a few tenths of millijanskys, respectively, in the next few years. This is an eminently feasible measurement, and could nicely constrain the current nucleus dichotomy (explained below, Section 2.2).

2.1.2. *Empirical Coma Fitting*

Since the radiometric method requires that one measure the brightness of the nucleus without any contaminating coma, it is necessary to separate the comatic and nuclear components of the cometary photometry. For some images of comets, it is possible to use an image processing technique that will let the observer account for this coma contamination. The technique, which models the surface brightness behavior of the coma in order to subtract it from the image, has been applied successfully to other comets by Lamy and co-workers (e.g., Lamy et al., 1998, 1999b) and Lisse et al. (1999). For Hale–Bopp, work on this has been done by Sekanina (1997a), Lamy et al. (1999a), and Fernández (1999).

The primary idea of this coma-fitting technique is to fit the power-law surface brightness profile of the coma at many azimuths in the image. These power laws are then extrapolated to the central pixels to make a synthetic image of the comet with coma only. The subtraction of the model from the original image leaves a

point source residual, which is the contribution from the nucleus. The method has four fundamental requirements. First, the point-spread function PSF must be well understood. This makes spacecraft observations, with their usually stable optics and seeing, the best choice. Second, the comet must show sufficient nucleus-vs.-coma contrast. The lower the contrast, the higher the signal-to-noise that is needed *in every pixel* (not just integrated) to be able to extract the nucleus. Third, the comet must show sufficient comatic surface brightness away from the photocenter to allow robust fitting. Fourth, the dust coma's surface brightness profile along any given azimuth must follow a single power law all the way to the nucleus's surface. For example, strongly curving jet features in the coma would usually defeat the method. This last requirement is somewhat difficult to confirm, so the closer the comet is to Earth, the more likely the technique is applicable. Virtually all of the Hale–Bopp work mentioned above has been done with 1995 and 1996 data, where spatial resolution is not optimum and there is concern that the inner coma environment is morphologically more complex than can be accounted by this formalism. Indeed the reported existence of a secondary, companion nucleus to Comet Hale–Bopp, claimed via adaptive-optics (Marchis et al., 1999) and via a technique similar to the one described here (Sekanina, 1997b), remains controversial because of the difficulty in understanding the inner coma's brightness distribution.

An example of the technique is shown in Figure 1, where an image from September 1995 (top left), taken by the Hubble Space Telescope (HST), has been analyzed by Weaver and Lamy (1997), who originally presented this figure. The upper right panel shows the coma model produced by the technique plus a point source that represents the nucleus. The difference of the top two panels is shown as an image in the lower left and as a radial profile in the lower right. Most of the flux has been removed, so this gives confidence that the comatic and nuclear components have been reliably constrained.

The application of this image processing technique to mid-IR Hale–Bopp data plays an important role in constraining R, and the data will be further discussed below (Section 2.2).

2.1.3. *Methods Not Requiring Thermal Behavior*

Occultations are frequently used to constrain the shape and size of asteroids. In principle the same can be done for comets except that an occultation trace could have wings due to any non-negligible optical depth in the inner coma, somewhat similar to that which is often seen in occultations of stars by objects with atmospheres (see work by Elliot and Olkin, 1996, for a review). However in practice this method is complicated by the astrometric difficulty of locating a tiny nucleus within a coma. Since subarcsecond errors in the sky position can translate into hundreds or thousands of kilometers of ground travel for the comet's shadow on Earth, only certain occultations by comets can be tried. Such a campaign to observe an occultation by Hale–Bopp was mounted in October 1996, and reported by Fernández et al. (1999). At the time, $r = 2.8$ AU and the comet had a significant

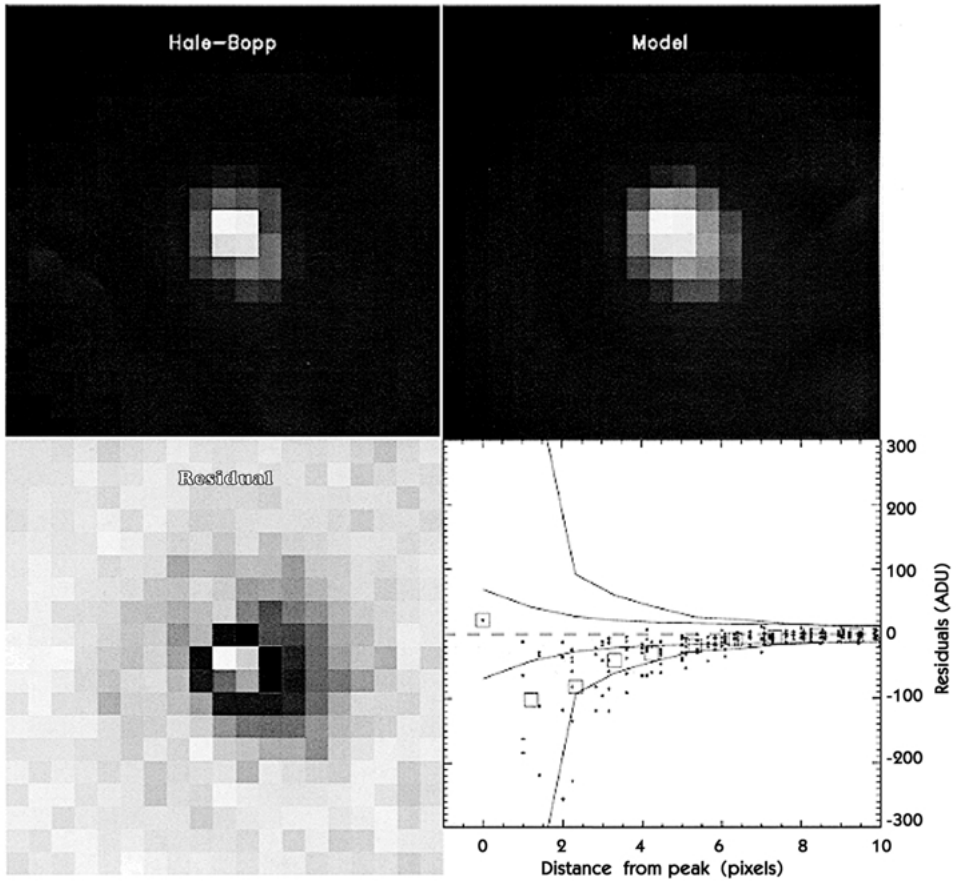

Figure 1. Demonstration of the coma fitting technique on an HST image of Hale–Bopp, as presented by Weaver and Lamy (1997). The upper left panel shows the original image. The upper right panel is the coma model created for that image plus a central point source that represents the nucleus. The difference of these two is in the lower left panel. Most of the flux has been accounted for, as can be seen by the profiles of the residual in the lower right panel. Plus-symbols are individual pixels, square-symbols are azimuthal averages, the inner pair of lines shows the 3-σ error estimates based on the standard CCD noise equation, and the outer pair of lines shows the 3-σ error estimates based on the scatter of the pixel values. Figure courtesy Hal Weaver.

dust coma, which made locating the nucleus's position difficult. One chord was measured that is consistent with a passage through an optically thick inner coma and possibly a small section of the nucleus itself. Without corroboration there is no way to be sure that this chord did pass through the inner coma but it is consistent with that scenario. The authors assumed a spherical nucleus and a hemispherically symmetric inner coma to derive an upper limit to the nucleus's size – $R < 26$ km. The results are model dependent.

Non-gravitational forces can in principle be used to determine the mass of a nucleus (and thence R given reasonable densities, or the density given R). The

parameterization of this effect was laid out via empirical formulae by Marsden (1969) and via physical arguments by Marsden et al. (1973). In the most basic form, this nongravitational acceleration times the nucleus's mass, is equal to the product of the mass loss rate and the outflow speed. However the answers depend very heavily on the location of the nucleus's active regions, the nucleus's shape, and the activity as a function of r. With Hale–Bopp, we are in the unusual position (compared to other long-period comets) of having gas and dust mass flux measurements over several years as well as imaging of the jet structure over a similarly long time period. Moreover we have some rough constraints on Hale–Bopp's nongravitational coefficients (Marsden, 1997). However at time of writing there has been no mass estimate presented based on this method.

Of course the best way to determine R is to simply take a spatially-resolved picture of the nucleus. This can be done *in situ*, as for comets 1P/Halley (Keller et al., 1986) and 19P/Borrelly (Soderblom et al., 2002), but it is unlikely that any spacecraft will visit Hale–Bopp in the near future. Another way is to use radar echoes, a technique whose application to asteroid studies burgeoned in the 1990s and continues onward. So far only a few comets have been detected with radar (Harmon et al., 1999), but the nuclei have either been too small or too far away to provide us with as stunning a set of "images" as we have of several near-Earth asteroids. Hale–Bopp never approached closer than $\Delta = 1.3$ AU and thus was an unsuitable radar target.

2.2. THE ANSWERS

The most definitive constraints on R are from mid-IR and radio measurements. Unfortunately, in the simplest interpretation, they give different results. Here we describe the data and then propose a possible reconciliation.

First there are the Infrared Space Observatory (ISO) ISOCAM measurements reported by Lamy et al. (1999a) and published by Jorda et al. (2000). The coma-fitting technique was applied by these workers and the resulting photometry, using the standard thermal model, gives an effective radius of 35 km. A more sophisticated "mixed model" (Lamy et al., 1999a; Groussin et al., 2000), a model of the comet as an ice/rock mixture, implies a cooler temperature for the nucleus and thus requires a larger radius; they report 56 km.

A possible complication here is that with Hale–Bopp being so active the subtraction of the coma's contribution may be difficult. With this premise, we constructed a simple model to further analyze the fluxes published by Jorda et al. (2000). We assumed that those fluxes have some small dust component remaining in them – that is, that the coma-fitting technique did not remove quite all of the dust in the photometry – and that the relative amounts of this remaining coma from wavelength to wavelength were the same as in the original dust spectral energy distribution.

Our model simply tries linear combinations of the dust component and the nuclear component to try to fit the published photometry. The dust coma spectrum published by Crovisier et al. (1997), which was taken with the SWS instrument on ISO at almost the same time as the ISOCAM data were obtained, was used as the dust template to provide us with the relative amount of flux from the dust at the relevant wavelengths. To make it appropriate for ISOCAM comparison, the spectrum was convolved through the relevant ISOCAM filters. For the nucleus's spectrum, we used the same "mixed model" results employed by Jorda et al. (2000). Thus our model has two parameters: the overall scale factor for the dust spectrum, and the radius of the nucleus. The result of this analysis is presented in Figure 2. The top panel shows the contour plot of the reduced χ^2 for 2 degrees of freedom. Note that the solution presented by Jorda et al. (2000), with a dust contribution of zero and a radius of 56 km, is an acceptable solution at the $\sim 1.5\sigma$ level. However the smallest χ^2 values reside in a region with a non-zero dust contribution and $0 < R < 50$ km. The bottom plot of the figure shows some possible dust+nucleus models that fit the data. The result of this exercise is that there is potentially considerable leeway in constraining the nucleus's size with the infrared data.

Moving on to the long-wavelength data, they are displayed in Figure 3. There are many radio measurements over the apparition but most of them were performed with telescopes that give too large a beam size to reliably extract a nuclear signature. In other words, most of the observations report dust coma instead of the nucleus. A few measurements however did have small enough beam sizes that it is reasonable to expect a significant contribution from the nucleus. Moreover many of these measurements were interferometric; such observations tend to suppress the large scale structure of the coma. The datasets that are plotted in the figure were those reported by de Pater et al. (1998), Altenhoff et al. (1999), Fernández (1999), and Qi (2000); they have been scaled to a common geocentric distance Δ, 1.317 AU, as Δ^2 and a common r, 0.93 AU, as $\sqrt{r}$. Since most of these measurements were made near perihelion, the adjustment for r, although rough, adds negligible additional uncertainty.

The solid line drawn through the points is our logarithmic fit to the five best-constrained points, and indicates that the flux density is best fit by a proportionality to the inverse-1.94-power of wavelength. In the Rayleigh-Jeans limit, an isothermal object with constant emissivity would be expected to emit flux density F_{radio} that follows the inverse-square of wavelength:

$$F_{radio} = \frac{2\pi kT}{\lambda^2}\epsilon(\lambda)\frac{R^2}{\Delta^2}, \tag{1}$$

where k is the Boltzmann constant, T is the temperature, λ is the wavelength, and ϵ is the emissivity as a function of wavelength. The data are consistent with this behavior, as the dotted line in the plot demonstrates. There is a subtlety here though, since these radio observations trace emission from subsurface layers of material,

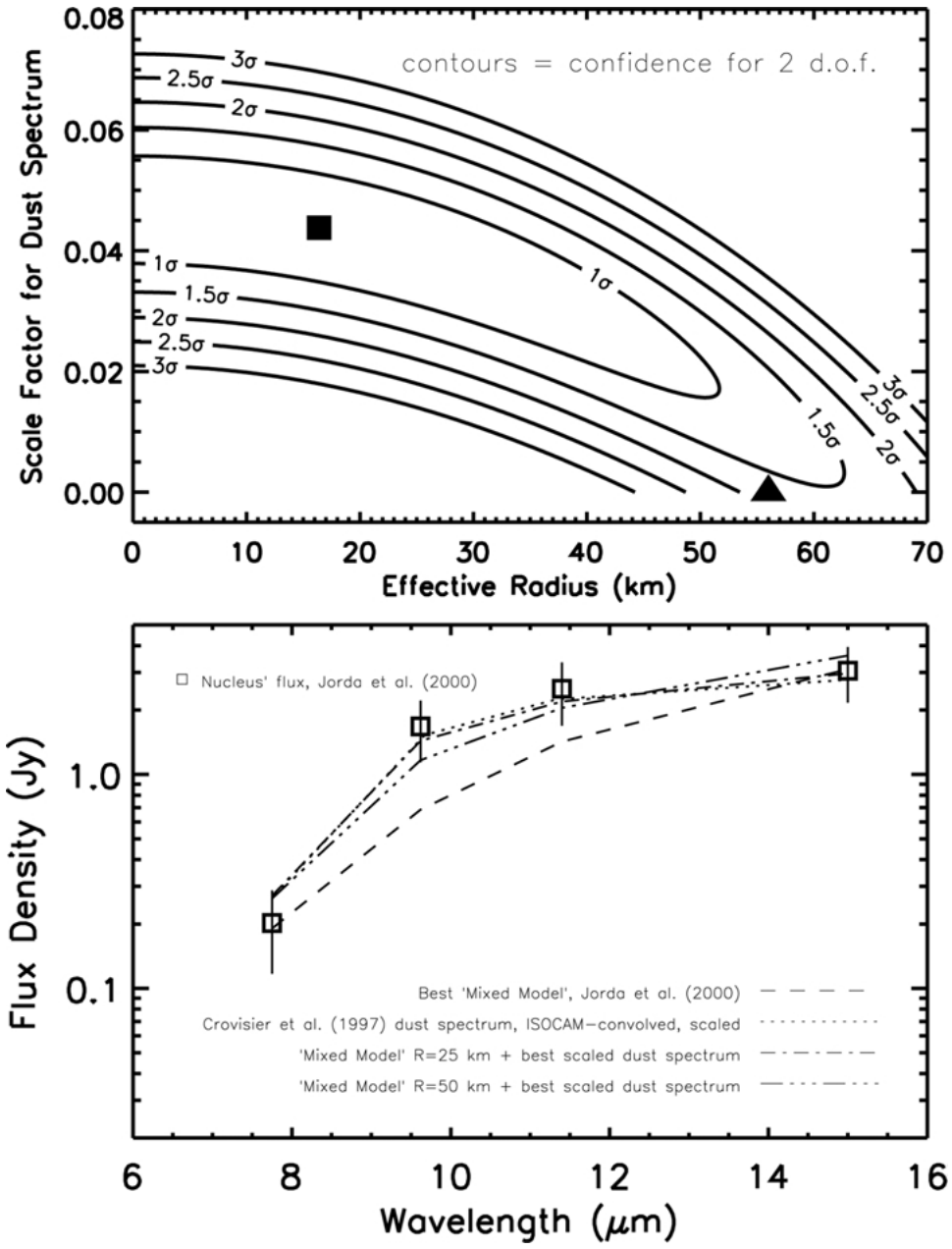

Figure 2. The possible remaining dust contribution to the coma-removed residuals published by Jorda et al. (2000). The top plot shows the contours of reduced χ^2 as converted to confidence levels for 2 degrees of freedom ("d.o.f."). A non-zero dust contribution is possible. The square marks the nominal location of the smallest χ^2. The triangle marks the result mentioned by Jorda et al. (2000). The bottom plot shows: The mixed-model nucleus (large-nucleus, no-dust) fit shown by Jorda et al. (2000); an all-dust, no-nucleus model, which is probably unphysical but nevertheless fits the data; and two feasible mixed-model plus dust spectrum models.

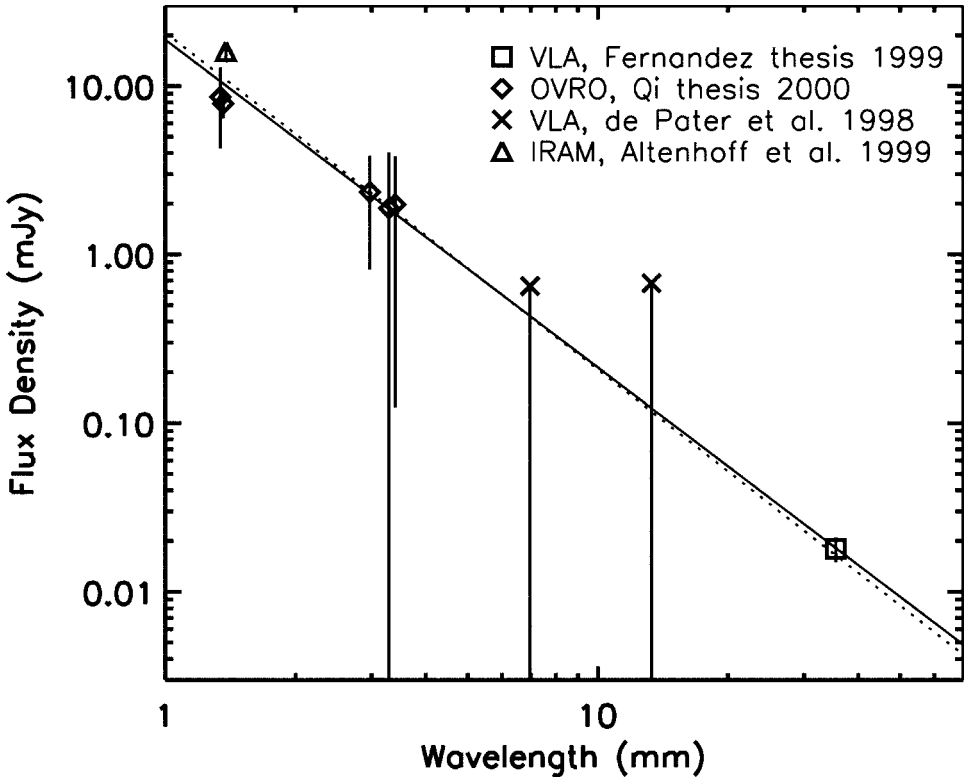

Figure 3. Radio photometry of Hale–Bopp's nucleus. Only the five best-constrained points were used to generate the best fitting power-law line (solid line). A λ^{-2} power-law is also shown (dotted line).

as opposed to the surface or near-surface material sampled by the mid-IR data. So it is worthwhile to consider T and ϵ more closely.

Regarding the temperature, by measuring the thermal continuum emitted below the surface, the radio data measure cooler temperatures and possibly a region less susceptible to the diurnal variation. For example a wavelength of 3.55 cm may be expected to sample up to a few decimeters beneath the surface, and up to a meter deep if there is a significant ice component (de Pater et al., 1983), whereas the diurnal thermal wave would only penetrate a few centimeters at most under most reasonable estimates of the thermal diffusivity.

Regarding the emissivity, for most infrared work ϵ is near unity and has little influence on the modeling results. Here we must use caution however since it is possible that at these wavelengths the emissivity is significantly smaller than 1. For example, Galilean satellites (Ostro, 1982), some Main Belt asteroids (Müller and Lagerros, 1998), and terrestrial glaciers (as noted by de Pater et al., 1983) all have radio emissivities much lower than unity (0.3, 0.6, and 0.5, respectively) at some wavelengths.

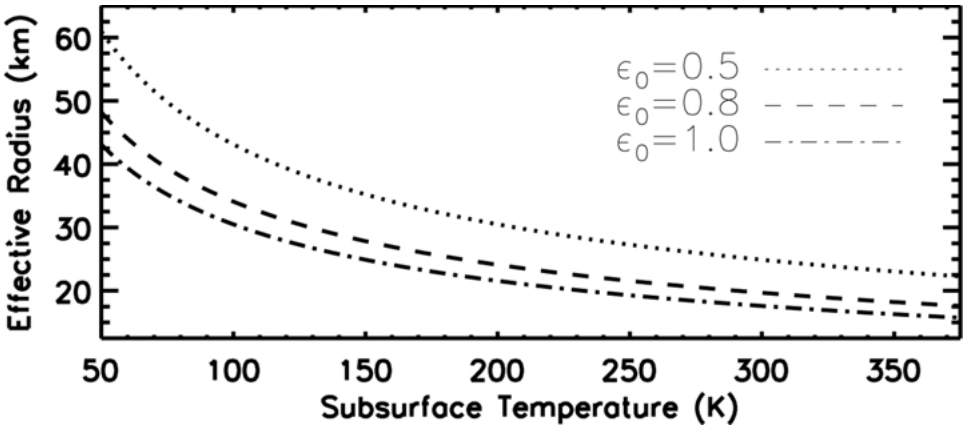

Figure 4. Constraints on the nucleus's size given the best λ^{-2} fit from Figure 3. Three values of ϵ_0 have been used to show the influence of that quantity. Effectively the radius depends on the thermal properties of the subsurface layer sampled by the radio data.

However we can be comforted by the apparent closeness of our fit to the λ^{-2} function over more than one decade in wavelength. If the emissivity were wildly changing, then we would not expect the nucleus's flux to follow so closely. For simplicity we can safely let $\epsilon(\lambda)$ equal a constant, ϵ_0. Furthermore, the depths sampled by the radio wavelengths differ by about an order of magnitude from one end of the measured continuum to the other. Presumably if there were a significant temperature difference between those layers, that would manifest itself in a continuum that deviates from λ^{-2}. A caveat is that the wavelength space is not well sampled and it is possible that we are being fooled: E.g., if the thermal behavior were pathological over the time frame of the observations and perhaps the sampled temperatures and the emissivity were varying in just the right way so that $T\epsilon$ would be constant but neither quantity alone would be.

Nevertheless we have some confidence in the applicability of our fit and we constrain the radius thus: $\epsilon_0 T R^2 = (9.3 \pm 2.9) \times 10^4$ K km^2, where the error bar marks the 1-σ confidence level based on a fit to the λ^{-2} law. Figure 4 shows how the value of R varies for given T and ϵ_0 according to this equation.

In Figure 4 one sees that it is possible for the radio data to be consistent with the Jorda et al. (2000) radius if the radial temperature gradient were extremely sharp, and the relevant subsurface layer were not much warmer than the cometary ices' probable formation temperature. The observed radical difference in jet activity between the day side and night side of 1P/Halley (Keller et al., 1986) and 19P/Borrelly (Soderblom et al., 2002) indicates that the thermal inertia and thermal conductivity into the nucleus is low, but it is probably not zero. For example, modeling of 1P/Halley's water production behavior constrains the thermal inertia within its active regions to be about 1 to 8 times that of the Moon (Julian et al.,

2000). Thus it is likely that the subsurface layer is not quite as cold as 30 to 50 K within the layer sampled by these data.

We can constrain the lower limit to the radius by assuming that the emissivity is unity and that the temperature can be no higher than that of a hypothetical isothermal surface. An isothermal, unit emissivity black body that is 0.93 AU from the Sun would have $T = 288$ K on the surface, and so R must be at least 18 km, based on Figure 4. Fortunately since R depends on the square root of the other quantities we can estimate its value with fairly good precision even allowing for a wide range of possible temperatures. For example $R = 25 \pm 5$ km if the emissivity is high and $125 \text{ K} < T < 275$ K. A conservative estimate would be $R = 30 \pm 10$ km, allowing for the same wide temperature range and an emissivity down to about 0.5. Note that these radii are consistent with our results shown in Figure 2 from the modeling of the ISO data.

In summary, the ISO and radio data can be reconciled if: (1) There is some excess, unremoved dust in the mid-IR spectrophotometry, which would lower that estimate of R; and (2) the subsurface layer sampled by the radio data is cooler and less emissive than expected, which would raise that estimate of R.

2.3. Context of Hale–Bopp's size

Table I gives a list of effective nuclear radii that have been constrained either radiometrically or via resolved imaging, in order of size. While Hale–Bopp is not the largest known cometary nucleus – Chiron is larger – it is certainly bigger than average. Note that we are still far from an observational sampling of the size distribution. For example in a differential size distribution proportional to $R^{-3.5}$ (i.e., collisional relaxation), there ought to be $5^{2.5} = 56$ times as many objects bigger than 1 km as there are objects bigger than 5 km. Attempts to tackle this problem are complicated by coma contamination, but several groups are working on it using compendia of visible-wavelength data (Fernández et al., 1999; Weissman and Lowry, 2001).

The large size of Hale–Bopp motivates us to discuss just how a comet with a large nucleus is different from the average. There are several properties that one might associate with having a large nucleus.

1. Albedo. Could there be any size-dependent variation of the albedo (or the color) due to say, the rate of mantling, or the physical mechanism of activity? A review by Campins and Fernández (2002) gives our current understanding of this topic.
2. Rotation. While there is some apparent difference in the distribution of rotation rates between comets and asteroids, there are too few known cometary periods to make a link with size. However, only comets larger than about 100 km in radius will have a damping timescale that is shorter than the spin-up time (Jewitt, 1997), so virtually all comets, even Hale–Bopp, can be in rotationally

TABLE I
Well-constrained cometary radii from radiometry and resolved imaging

Object	R (km)	Ref.
95P/Chiron	80 ± 10	1
C/1995 O1 Hale–Bopp	30 ± 10	2
28P/Neujmin 1	10.0 ± 0.5	3
10P/Tempel 2	$5.9 \begin{smallmatrix} + & 0.25 \\ - & 0.7 \end{smallmatrix}$	4
49P/Arend–Rigaux	5.1 ± 0.25	5
1P/Halley	5.0	6
C/1983 H1 IRAS-Araki–Alcock	4.6	7
9P/Tempel 1	2.6 ± 0.3	8
2P/Encke	2.4 ± 0.3	9
C/1996 B2 Hyakutake	2.25 ± 0.3	10
19P/Borrelly	2.2	11
107P/Wilson–Harrington	1.95 ± 0.25	12
55P/Tempel–Tuttle	1.7 ± 0.3	13, 14
22P/Kopff	1.52	14
126P/IRAS	1.43	14
103P/Hartley 2	0.58	14

References: (1) Campins et al., 1994 and Fernández et al., 2002; (2) this work; (3) Campins et al., 1987; (4) A'Hearn et al., 1989; (5) Millis et al., 1988; (6) cube root of 3 axial dimensions given by Keller et al., 1986; (7) cube root of 3 axial dimensions given by Sekanina, 1988; (8) own work; (9) Fernández et al., 2000; (10) Sarmecanic et al., 1997 and Lisse et al., 1999; but see Harmon et al., 1997; (11) cube root of estimated axial dimensions from results presented by Soderblom et al., 2002; (12) Campins et al., 1995; (13) Fernández, 1999; (14) Jorda et al., 2000.

excited states due to their outgassing. A review of this phenomenon is given by Samarasinha and Belton (1995).

3. Internal Structure. The effects of radiogenic heating become more important for larger objects. A review by Prialnik (2002) gives our current understanding of this topic.

4. Bound Atmosphere. So far, apparently Chiron is the only comet big enough to have a bound atmosphere (Meech et al., 1997). Hale–Bopp is probably not quite large enough for this phenomenon to play a role. The requirements for a Centaur or trans-Neptunian object to have a bound coma have been investigated by Brown and Luu (1998).

5. Activity. It is possible to make a gross association that, all else being equal (most importantly active fraction), bigger comets will be more active. This topic will be considered in more detail in the next section.

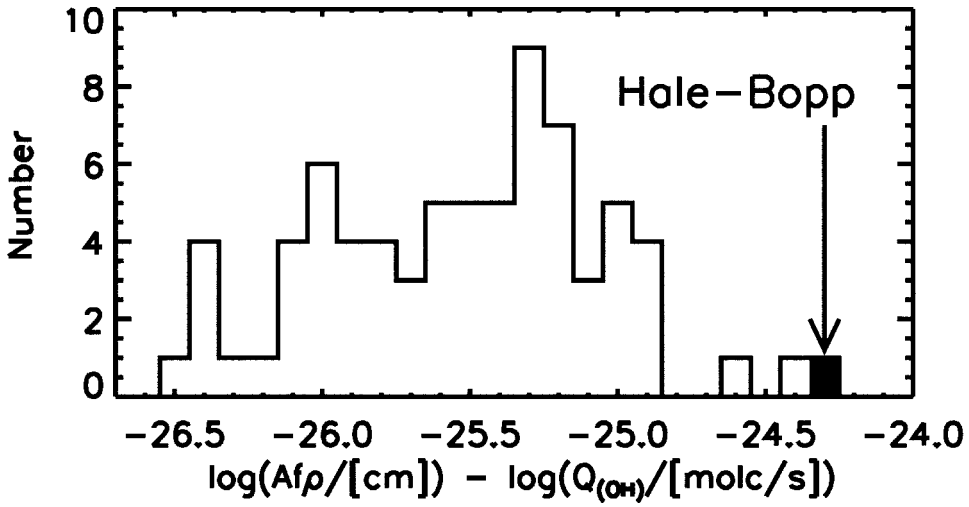

Figure 5. A comparison of Hale–Bopp's dust-to-gas ratio with the compilation published by A'Hearn et al. (1995). For Hale–Bopp, values obtained by Farnham et al. (1997) are shown since the same methodology was used: photometry at visible wavelengths. The comet adjacent to Hale–Bopp on the plot is Shoemaker–Levy C/1991 B1.

3. Activity

There are many aspects related to Hale–Bopp's fecund output of dust that could be discussed, but in the interest of brevity only a few topics will be covered here. To understand the relationship of Hale–Bopp to the ensemble of comets, Figure 5 places the comet's mass loss rate in perspective. Hale–Bopp has the highest dust-to-gas ratio known in addition to having the highest peak mass loss rate and the highest total mass loss (excepting catastrophically disintegrating comets). The comet has been active since discovery; furthermore, a pre-discovery image from 1993 (McNaught, 1995) shows that the comet has been active for at least 9 years so far. For reference, the perihelion dust production rate of the comet was 2×10^6 kg/s from sub-mm measurements (Jewitt and Matthews, 1999), 5×10^5 kg/s from mid-IR measurements (Lisse et al., 1997), and $1 - 2 \times 10^5$ kg/s from visible-wavelength measurements (Farnham et al., 1997; Weaver et al., 1999). This production rate varied as r^{-1} to r^{-2} (Schleicher et al., 1997; Lisse et al., 1997; Weaver et al., 1997).

3.1. Jets over time

A very dramatic feature of Hale–Bopp's activity was the evolving, prominent set of jets. A display of the major features is shown in Figure 6, with original images in the top row and their processed counterparts on the bottom. In 1995, after discovery, the comet showed us quasi-periodic outbursts that produced spiral-shaped structures lasting for several days (left images). By mid- and late-1996, the jets

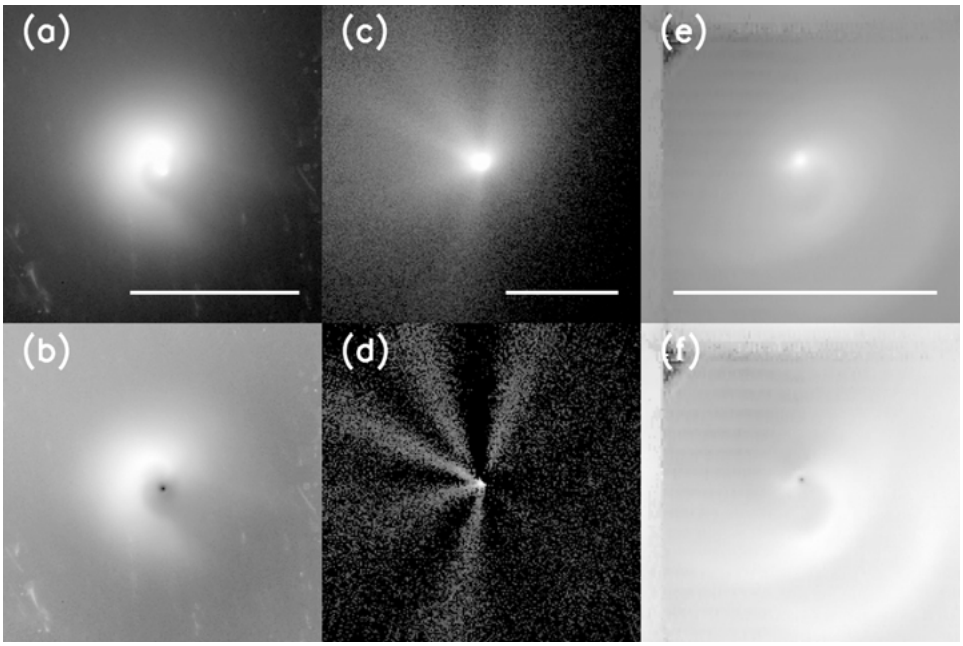

Figure 6. The variation in jet structure over the course of Hale–Bopp's apparition. In each frame the white bar represents 50,000 km at the comet. (a) Transient spiral jets, lasting a few days, were common in 1995; figure courtesy Hal Weaver and HST Archive. (b) Processed image ($1/\rho$ coma removed) to enhance the jet features. (c) Linear stationary jets dominated in late 1996; figure courtesy Ron Stone. (d) Processed image (rotational-shift-differencing) to enhance the jet features. (e) Near perihelion in early 1997 a spiral jet rotating with an 11.3-hour period was visible; figure courtesy Casey Lisse. (f) Processed image ($1/\rho$ coma removed) to enhance the jet features.

had transformed into linear features with remarkable stability (middle images), prompting the sobriquet of "porcupine" (Manzini et al., 1996). The features were thought to be caused by the optical depth effect of looking through a conical section of ejected dust (Sekanina and Boehnhardt, 1997; Boehnhardt et al., 1997); three or four active areas were outgassing on the nucleus's surface at the time. After the 1997 solar conjunction, the comet reappeared with yet another morphology, the rapidly-spinning spiral jet (right images). In fact there were several jets identified in 1997; the one shown in the figure was the brightest just after perihelion. Here the morphology let many groups finally pin down the dominant rotation period of about 11.3 hours (e.g., Jorda et al., 1997; Licandro et al., 1997). One should note that this discussion only refers to the dust jets, and that the comet showed *gas* jets wholly unassociated with the dust, and moreover these jets could be traced through the full 360° of position angle (Lederer, 2000).

A significant literature exists on many attempts to provide a "grand unified theory" for the jet features throughout the apparition. Such a model must incorporate a rotation axis that is not suffering from drastic precession; constraints on any migration of the rotation axis about the angular momentum vector are very

strict (Samarasinha et al., 1997; Licandro et al., 1998; Molina and Moreno, 1999). Among several models, two promising ones are described here.

Samarasinha (2000) has found a rotation direction and a model that satisfies both the 1996 and 1997 morphologies. An active region produces easily-resolvable, expanding helical structures near perihelion, but the larger geocentric distance in 1996 would let an observer only see linear features that are the borders of the cone of activity. This is a similar conclusion to that adopted by Boehnhardt et al. (1997). One of the very important discoveries by Samarasinha (2000) is the strong influence that the size of a jet's footpoint on the surface can have on the jet's shape in the coma. For example, a very broad footpoint is required to explain the apparent ellipticity of the prominent, near-perihelion spiral (Figure 6e). Narrow jets, such as one that might come from a deep vent on the surface, cannot explain the spirals without resorting to unphysical rotational behavior. This immediately implies that a significant area on (and thus a significant fraction of) Hale–Bopp's surface was active. Schleicher et al. (1997) calculate 930 km^2, which is about 5 to 20 percent of the surface area, a percentage comparable to that of 1P/Halley.

Recently Farnham et al. (IAU Coll. 186, Tenerife and private communication) have presented intriguing results that can explain not only the prominent, near-perihelion spiral jet shown in Figure 6 but also the multiple-jet morphology seen earlier in 1997 as well as the overall surface brightness contrast between the jet and the diffuse coma component. Their model implies that the rotation axis is pointing several tens of degrees away from the consensus direction reached earlier (e.g., Jorda et al., 1997; Licandro et al., 1997; Samarasinha et al., 1997; Vasundhara and Chakraborty, 1999).

In any case the rich variety of jet activity shown by Hale–Bopp has given us a way to probe the nature of its activity and its rotation, and there is confidence that a complete understanding will be at hand in the near future.

3.2. Optical depth

A calculation done by Weaver and Lamy (1997) showed how the space density of dust in the vicinity of the nucleus was high enough to possibly make Hale–Bopp's inner coma optically thick in visible wavelengths. For a given dust production rate the maximum value of the optical depth τ is inversely correlated with R, since the volume of space just adjacent to the nucleus is larger. Since the dust production varies roughly as R^2, however, on the average the maximum τ will be larger for larger nuclei (Müller, M., Green, S. F., and McBride, N.: 2002, these proceedings), and indeed there is some circumstantial, observational evidence that Hale–Bopp carried an optically thick inner coma: the occultation results reported by Fernández et al. (1999). They measured a chord apparently through the comet's coma that would imply a significant optical depth: > 1 within roughly 100 km of the nucleus's center. Thus perhaps Hale–Bopp's nucleus was shrouded by a shell of optically thick dust.

There are two significant manifestations of an optically thick inner coma. First is the question of how sunlight penetrates to the nucleus to heat the surface and drive the sublimation and activity. There are several published analyses (e.g., Weissman and Kieffer, 1981; Salo, 1988) on the contribution by the coma itself in providing energy to the nucleus's surface. In an optically thick inner coma the scattered light component would be diminished but the reradiated component would be substantial. This is especially true for the superheated coma; Hale–Bopp's significant population of sub-micron grains were heated well in excess of the local, equilibrium black-body temperature (Mason et al., 2001).

Second, an optically thick coma complicates our interpretation of the size of the nucleus. The radio data are probably the most immune to this problem, since at those wavelengths very large grains would be needed, grains which are thought to not contribute much radiating surface area (compared to the more abundant micron and sub-micron grains). A potentially more problematic scenario exists with the visible data however, such as those shown in Figure 1. The coma-fitting may be very nicely extracting the cross section of the optically-thick dust shell instead of the cross section of the nucleus. Since HST provided some of the highest spatial resolution data at the visible wavelengths, it may bode ill for reliable nuclear size/albedo information to be extracted from visible datasets.

The very high albedo of Hale–Bopp's dust (Mason et al., 2001) may offer a way to mitigate the problem, however. To zeroth order the light from the extracted "nucleus" (such as done in Figure 1) is proportional to $a^2 N A_d + R^2 p e^{-\tau}$, where a is the "typical" grain radius in the optically-thick shell, N is the effective number of these grains within one optical depth, and A_d is the albedo of the dust. A rough upper limit to the value of p can be estimated by assuming that the extraction has revealed only nucleus; the answer, $p \approx 0.045$ (Fernández, 1999; Jorda et al., 2000), is in line with other nuclear albedos. Now, since A_d is so high compared to p, possibly by as much as an order of magnitude, the value of p is sensitive to the relative contributions of the two terms. If the first term were overwhelmingly dominating, then p would have to be infeasibly low (since we probably have reasonable estimates of R and τ). Thus, while the optically thick shell is certainly contributing to visible-wavelength photometry of the near-nucleus region, it probably cannot be the dominant term.

3.3. Interplanetary dust environment

Kresák and Kresáková (1987) calculated that the short-period (SP) comet population provided about 3×10^{12} kg of dust into bound orbits about the Sun per century. This is the source of a significant fraction of the interplanetary dust environment (i.e., the interplanetary dust particle, or IDP, population). The Main Asteroid Belt provides most of the remainder. This calculation was done using only visible-wavelength studies of cometary dust, and since only the micron and sub-micron grains are optically sensitive at those wavelengths, this underestimates the total

contribution; it is reasonable to estimate that the true amount is around 3×10^{13} to 10^{14} kg.

Using the numbers quoted at the start of Section 3, we can integrate Hale–Bopp's dust production rate over its entire orbit and find that the comet ejects roughly 3×10^{13} kg per apparition (Jewitt and Matthews, 1999), i.e., approximately the same amount as the *total* SP contribution in 100 years. Thus one may ask what contribution the long-period (LP) comets make to the IDP population.

The caveat is that only the largest grains released by LP comets stay bound in the Solar System. Smaller grains go into unbound, hyperbolic orbits as a result of the radiation pressure and the orbital speed with which they start. The cutoff grain size is approximately 1 mm (Lisse et al., 1998). This phenomenon diminishes the LP contribution of IDPs since most LP comets are not productive enough to eject a significant number of such large grains.

However we now have Hale–Bopp, whose mass loss was larger than virtually all other known LP comets. The comet's grain size distribution is shown in the top panel of Figure 7. The curve belongs to 1P/Halley's dust grain size distribution but it is thought to be applicable to Hale–Bopp (Hanner et al., 1997; Lisse et al., 1997) as well. The middle plot shows the curve converted to a mass distribution, and the final plot shows the running integral of total mass. The scales of all three curves have been set so that they approximately match the total Hale–Bopp mass loss. Clearly most of the mass leaves Hale–Bopp in the form of the large millimeter and centimeter grains. Thus, since Hale–Bopp is such a prodigious producer of these grains, this comet can in fact make a non-negligible contribution to replenishing the IDP population.

Only LP comets with dust production rates comparable to that of Hale–Bopp are important for this effect, but nevertheless this cometary group can be considered as a third source of IDPs. If the comets as a whole provide about half of the total IDP mass, and we have 1 Hale–Bopp-class comet per century, then the long period comets provide roughly a few percent of the IDP population.

4. Summary

The state of research regarding the size of Hale–Bopp has been presented. The best datasets for constraining the problem reside with the measurements made by ISO+ISOCAM in late 1996 in the mid-IR and the multiple radio measurements made near perihelion. Unfortunately, to first order, the two wavelength regimes give different results. However, the former dataset could suffer from incomplete coma subtraction and the latter dataset could suffer from sampling a lower emissivity and a cooler subsurface temperature. A possible solution is presented that reconciles the measurements in the two regimes: an effective radius of 30 ± 10 km is posited as a compromise.

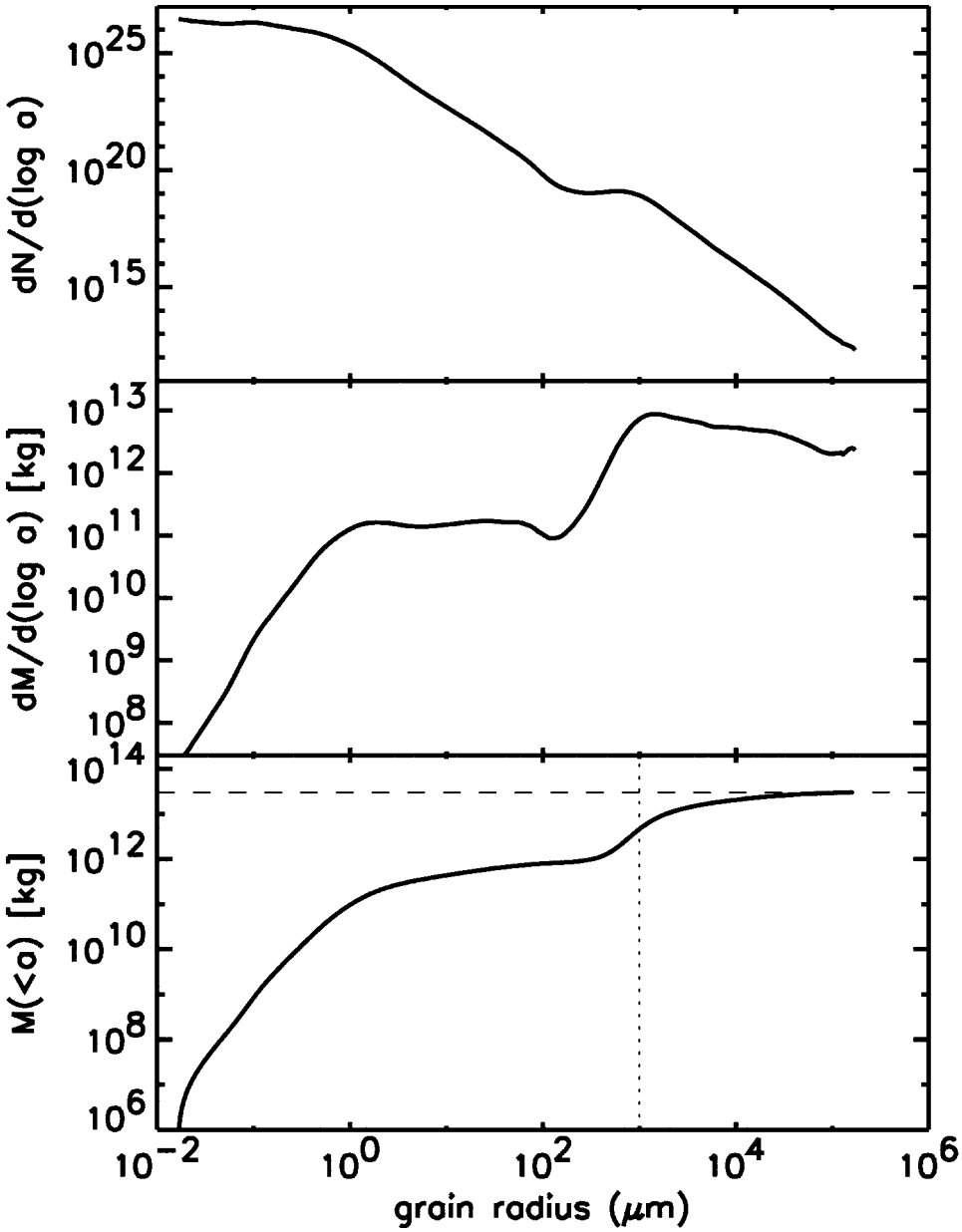

Figure 7. An estimate of the large particle mass contribution to the interplanetary dust environment by Hale–Bopp. The top plot shows the McDonnell et al. (1991) dust size distribution, the middle panel shows the mass distribution, and the bottom panel shows the total mass ejected as a function of biggest grain size. The plots were scaled to approximately match Hale–Bopp's estimated total mass output. It is clear from the bottom plot that most of the mass comes out in grains that are millimeter-scale and larger (vertical dotted line). This compares with the roughly $10^{13.5}$ kg total contribution from the SP comets (horizontal dashed line).

In comparison to the other nuclear radii that have been radiometrically constrained, Hale–Bopp's nucleus is second only to Chiron's. This large size motivates one to ponder what other properties about the comet are tied to the nucleus's size and thus "make a big comet different". Many interesting topics are possible but the aspects of the dust activity are chosen, specifically: the jet morphology, the dust opacity, and the relationship with the interplanetary dust environment.

Hale–Bopp's rich jet morphology can be at least partially explained by jets with very wide footpoints on the surface; this large nucleus had a large active area and a large active fraction. A unified model of rotation and jet activity is currently being formulated by several groups to explain all the coma features seen in 1995, 1996, and 1997.

The optical depth of the dust was likely near unity in the inner coma. While there is little observational evidence for this phenomenon, if true it could pose problems for extracting information on the nuclear size from visible-wavelength data. What would be thought of as the signature of the "nucleus" could actually be just the optically-thick dust shell. However, given the brightness of these signatures and reasonable albedos for a nucleus, such a dust shell is probably contributing but not dominating the measured flux.

The dust from most long-period comets cannot stay in the interplanetary dust environment since most grains are put on unbound, hyperbolic orbits once they leave the nucleus. However Hale–Bopp is different. Since its dust production was so prodigious, it ejected a significant number of millimeter and centimeter-sized grains, grains that are in fact large enough to stay on bound orbits about the Sun. The total mass of these large grains is a non-negligible fraction of the contribution that all short-period comets provide in a century. Thus Hale–Bopp was one of the rare long-period comets to appreciably replenish some of the interplanetary dust environment.

Acknowledgements

The author appreciates the financial support of the I.A.U. and N.A.S.A. (through a grant to David C. Jewitt) to attend the conference where this paper was first presented, and the terrific logistical support that Dr. S. B. Peschke provided before the presentation. Drs. D. C. Jewitt, K. J. Meech, C. M. Lisse, and L. M. Woodney provided helpful comments to improve this paper's quality.

References

A'Hearn, M. F., Campins, H., Schleicher, D. G., and Millis, R. L.: 1989, 'The Nucleus of Comet P/Tempel 2', *Ap. J.* **347**, 1155–1166.

A'Hearn, M. F., Millis, R. L., Schleicher, D. G., Osip, D. J., and Birch, P. V.: 1995, 'The Ensemble Properties of Comets: Results from Narrowband Photometry of 85 Comets: 1976–1992', *Icarus* **118**, 223–270.

Allen, D. A.: 1970, 'Infrared Diameter of Vesta', *Nature* **227**, 158–159.

Altenhoff, W. J., Bieging, J. H., Butler, B., Butner, H. M., Chini, R., Haslam, C. G. T., Kreysa, E., Martin, R. N., Mauersberger, R., McMullin, J., Muders, D., Peters, W. L., Schmidt, J., Schraml, J. B., Sievers, A., Stumpff, P., Thum, C., von Kap-Herr, A., Wiesemeyer, H., Wink, J. E., and Zylka, R.: 1999, 'Coordinated Radio Continuum Observations of Comets Hyakutake and Hale–Bopp from 22 to 860 GHz', *A. & A.* **348**, 1020–1034.

Boehnhardt, H., Birkle, K., Fiedler, A., Jorda, L., Peschke, S., Rauer, H., Schulz, R., Schwehm, G., Thomas, N., Tozzi, G., and West, R.: 1997, 'Dust Morphology of Comet Hale–Bopp (C/1995 O1): I. Pre-Perihelion Coma Structures in 1996', *Earth Moon Planets* **78**, 179–187.

Brown, W. R., and Luu, J. X.: 1998, 'Properties of Model Comae around Kuiper Belt and Centaur Objects', *Icarus* **135**, 415–430.

Campins, H., A'Hearn, M. F., and McFadden, L. A.: 1987, 'The Bare Nucleus of Comet Neujmin 1', *Ap. J.* **316**, 847–857.

Campins, H. and Fernández, Y.: 2002, 'Observational Constraints on Surface Characteristics of Comet Nuclei', these proceedings.

Campins, H., Osip, D. J., Rieke, G. H., and Rieke, M. J.: 1995, 'Estimates of the Radius and Albedo of Comet-Asteroid Transition Object 4015 Wilson–Harrington Based on Infrared Observations', *Planet. Space Sci.* **43**, 733–736.

Campins, H., Telesco, C. M., Osip, D. J., Rieke, G. H., Rieke, M. J., and Schulz, B.: 1994, 'The Color Temperature of (2060) Chiron: A Warm and Small Nucleus', *A.J.* **108**, 2318–2322.

Cowan, J. J., and A'Hearn, M. F.: 1979, 'Vaporization of Comet Nuclei – Light Curves and Life Times', *Moon Planets* **21**, 155–171.

Crovisier, J., Leech, K., Bockelée-Morvan, D., Brooke, T. Y., Hanner, M. S., Altieri, B., Keller, H. U., and Lellouch, E.: 1997, 'The Spectrum of Comet Hale–Bopp (C/1995 01) Observed with the Infrared Space Observatory at 2.9 AU from the Sun', *Science* **275**, 1904–1907.

de Pater, I., Forster, J. R., Wright, M., Butler, B. J., Palmer, P., Veal, J. M., A'Hearn, M. F., and Snyder, L. E.: 1998, 'BIMA and VLA Observations of Comet Hale–Bopp at 22–115 GHz', *A.J.* **116**, 987–996.

de Pater, I., Wade, C. M., Houpis, H. L. F., and Palmer, P.: 1983, 'The Nondetection of Continuum Radiation from Comet IRAS–Araki–Alcock (1983d) at 2- to 6-cm Wavelengths and its Implication on the Icy-Grain Halo Theory', *Icarus* **62**, 349–359.

Dello Russo, N., Mumma, M. J., DiSanti, M. A., Magee-Sauer, K., Novak, R., and Rettig, T. W.: 2000, 'Water Production and Release in Comet C/1995 O1 Hale–Bopp', *Icarus* **143**, 324–337.

DiSanti, M. A., Mumma, M. J., Dello Russo, N., Magee-Sauer, K., Novak, R., and Rettig, T. W.: 1999, 'Identification of Two Sources of Carbon Monoxide in Comet Hale–Bopp', *Nature* **399**, 662–665.

Elliot, J. L. and Olkin, C. B.: 1996, 'Probing Planetary Atmospheres with Stellar Occultations', *Annu. Rev. Earth Planet. Sci.* **24**, 89–123.

Farnham, T., Schleicher, D., and Lederer, S.: 1997, 'Comet C/1995 O1 (Hale–Bopp)', *IAU Circ.* **6589**.

Fernández, J. A., Tancredi, G., Rickman, H., and Licandro, J.: 1999, 'The Population, Magnitudes, and Sizes of Jupiter Family Comets', *A. & A.* **352**, 327–340.

Fernández, Y. R.: 1999, 'Physical Properties of Cometary Nuclei', Ph.D. Thesis, University of Maryland, College Park.

Fernández, Y. R., Jewitt, D. C., and Sheppard, S. S.: 2002, 'Thermal Properties of Centaurs Asbolus and Chiron', *A.J.* **123**, 1050–1055.

Fernández, Y. R., Lisse, C. M., Käufl, H. U., Peschke, S. B., Weaver, H. A., A'Hearn, M. F., Lamy, P. L., Livengood, T. A., and Kostiuk, T.: 2000, 'Physical Properties of the Nucleus of Comet 2P/Encke', *Icarus* **147**, 145–160.

Fernández, Y. R., Wellnitz, D. D., Buie, M. W., Dunham, E. W., Millis, R. L., Nye, R. A., Stansberry, J. A., Wasserman, L. H., A'Hearn, M. F., Lisse, C. M., Golden, M. E., Person, M. J., Howell, R. R., Marcialis, R. L., and Spitale, J. N.: 1999, 'The Inner Coma and Nucleus of Hale–Bopp: Results from a Stellar Occultation', *Icarus* **140**, 205–220.

Groussin, O., Peschke, S., and Lamy, P. L.: 2000, 'Properties of 2060 Chiron from Infrared ISOPHOT Observations', *Bull. Amer. Astron. Soc.* **32**, 1031–1031.

Hainaut, O., West, R. M., Marsden, B. G., Smette, A., and Meech, K.: 1995, 'Post-Perihelion Observations of Comet P/Halley. IV. r=16.6 and 18.8 AU', *A. & A.* **293**, 941–947.

Hanner, M. S., Gehrz, R. D., Harker, D. E., Hayward, T. L., Lynch, D. K., Mason, C. C., Russell, R. W., Williams, D. M., Wooden, D. H., and Woodward, C. E.: 1997, 'Thermal Emission from the Dust Coma of Comet Hale–Bopp and the Composition of the Silicate Grains', *Earth Moon Planets* **79**, 247–264.

Harmon, J. K., Campbell, D. B., Ostro, S. J., and Nolan, M. C.: 1999, 'Radar Observations of Comets', *Planet. Space Sci.* **47**, 1409–1422.

Harmon, J. K., Ostro, S. J., Benner, L. A. M., Rosema, K. D., Jurgens, R. F., Winkler, R., Yeomans, D. K., Choate, D., Cormier, R., Giorgini, J. D., Mitchell, D. L., Chodas, P. W., Rose, R., Kelley, D., Slade, M. A., and Thomas, M. L.: 1997, 'Radar Detection of the Nucleus and Coma of Comet Hyakutake (C/1996 B2)', *Science* **278**, 1921–1922.

Harris, W. M., Morgenthaler, J. P., Scherb, E., Anderson, C., and Oliversen, R. J.: 2002, 'Wide Field Imaging and the Velocity Structure in the Coma of Hale–Bopp', these proceedings.

Jewitt, D.: 1991, 'Cometary Photometry', in R. L. Newburn, Jr., M. Neugebauer, and J. Rahe (eds.), *Comets in the Post-Halley Era*, Kluwer Academic Publishers, Dordrecht.

Jewitt, D.: 1997, 'Cometary Rotation', *Earth Moon Planets* **79**, 35–53.

Jewitt, D. and Matthews, H.: 1999, 'Particulate Mass Loss from Comet Hale–Bopp', *A.J.* **117**, 1056–1062.

Jorda, L., Lamy, P., Groussin, O., Toth, I., A'Hearn, M. F., and Peschke, S.: 2000, 'ISOCAM Observations of Cometary Nuclei', in R. J. Laureijs, K. Leech, and M. F. Kessler (eds.), *ESA SP-455: ISO Beyond Point Sources*, European Space Agency, Noordwijk.

Jorda, L., Rembor, K., Lecacheux, J. Colom, P., Colas, F., Frappa, E., and Lara, L. M.: 1997, 'The Rotational Parameters of Hale–Bopp (C/1995 O1) from Observations of the Dust Jets At Pic du Midi Observatory', *Earth Moon Planets* **77**, 167–180.

Julian, W. H., Samarasinha, N. H., and Belton, M. J. S.: 2000, 'Thermal Structure of Cometary Active Regions: Comet 1P/Halley', *Icarus* **144**, 160–171.

Keller, H. U., Arpigny, C., Barbieri, C., Bonnet, R. M., Cazes, S., Coradini, M., Cosmovici, C. B., Delamere, W. A., Huebner, W. F., Hughes, D. W., Jamar, C., Malaise, D., Reisema, H. J., Schmidt, H. U., Schmidt, W. K. H., Seige, P., Whipple, F. L., and Wilhelm, K.: 1986, 'First Halley Multicolour Camera Imaging Results from Giotto', *Nature* **321**, 320–326.

Kidger, M. R.: 1997, 'Dust Activity in Comet Hale–Bopp', *Earth Moon Planets* **79**, 79–102.

Kresák, L. and Kresáková, M.: 1987, 'The Mass Loss Rate of Periodic Comets', in B. Battrick (eds.), *Diversity and Similarity in Comets*, European Space Agency, Noordwijk.

Lamy, P. L., Jorda, L., Toth, I., Groussin, O., A'Hearn, M. F., and Weaver, H. A.: 1999a, 'Characterization of the Nucleus of Comet Hale–Bopp from HST and ISO Observations', *Bull. Amer. Astron. Soc.* **31**, 1116–1116.

Lamy, P. L., Toth, I., A'Hearn, M. F., and Weaver, H. A.: 1999b, 'Hubble Space Telescope Observations of the Nucleus of Comet 45P/Honda–Mrkos–Pajdusakova and its Inner Coma', *Icarus* **140**, 424–438.

Lamy, P. L., Toth, I., and Weaver, H. A.: 1998, 'Hubble Space Telescope Observations of the Nucleus and Inner Coma of Comet 19P/1904 Y2 (Borrelly)', *A. & A.* **337**, 945–954.

Lebofsky, L. A. and Spencer, J. S.: 1989, 'Radiometry and Thermal Modeling of Asteroids', in R. P. Binzel, T. Gehrels, and M. S. Matthews (eds.), *Asteroids II*, University of Arizona Press, Tucson.

Lederer, S. M.: 2000, 'The Chemical and Physical Properties of the OH, CN, and C_2 Jets in Comet Hale–Bopp (1995 O1)', Ph.D. Thesis, University of Florida.

Licandro, J., Bellot Rubio, L. R., Boehnhardt, H., Casas, R., Goetz, B., Gómez, A., Jorda, L., Kidger, M. R., Osip, D., Sabalisck, N., Santos, P., Serra-Ricart, M., Tozzi, G. P., and West, R.: 1998, 'The Rotation Period of C/1995 O1 (Hale–Bopp)', *Ap. J.* **501**, L221–L225.

Licandro, J., Bellot Rubio, L. R., Casas, R., Gómez, A., Kidger, M. R., Sabalisk, N., Santos-Sanz, P., Serra-Ricart, M., Torres-Chico, R., Oscoz, A., Jorda, L., and Denicolo, G.: 1997, 'The Spin Axis Position of C/1995 O1 (Hale–Bopp)', *Earth Moon Planets* **77**, 199–206.

Lisse, C. M., A'Hearn, M. F., Hauser, M. G., Kelsall, T., Lien, D. J., Moseley, S. H., Reach, W. T., and Silverberg, R. F.: 1998, 'Infrared Observations of Comets by COBE', *Ap. J.* **496**, 971–991.

Lisse, C. M., Fernández, Y. R., A'Hearn, M. F., Kostiuk, T., Livengood, T., Käufl, H. U., Hoffmann, W. F., Dayal, A., Ressler, M. E., Hanner, M. S., Fazio, G. G., Hora, J. L., Peschke, S. B., Grün, E., and Deutsch, L. K.: 1997, 'Infrared Observations of Dust Emission from Comet Hale–Bopp', *Earth Moon Planets* **78**, 251–257.

Lisse, C. M., Fernández, Y. R., Kundu, A., A'Hearn, M. F., Dayal, A., Deutsch, L. K., Fazio, G. G., Hora, J. L., and Hoffmann, W. F.: 1999, 'The Nucleus of Comet Hyakutake (C/1996 B2)', *Icarus* **140**, 189–204.

Manzini, F., Guaita, C., and Crippa, F.: 1996, 'Comet C/1995 O1 (Hale–Bopp)', *IAU Circ.* **6463**.

Marchis, F., Boehnhardt, H., Hainaut, O. R., and Le Mignant, D.: 1999, 'Adaptive Optics Observations of the Innermost Coma of C/1995 O1. Are There a "Hale" and a "Bopp" in Comet Hale–Bopp?', *A. & A.* **349**, 985–995.

Marsden, B. G.: 1969, 'Comets and Nongravitational Forces. II.', *A.J.* **74**, 720–734.

Marsden, B. G.: 1997, 'Orbit Evolution and Evolution of Comet C/1995 O1 (Hale–Bopp)', *Earth Moon Planets* **79**, 3–15.

Marsden, B. G., Sekanina, Z., and Yeomans, D. K.: 1973, 'Comets and Nongravitational Forces. V.', *A.J.* **78**, 211–225.

Mason, C. G., Gehrz, R. D., Jones, T. J., Woodward, C. E., Hanner, M. S., and Williams, D. M.: 2001, 'Observations of Unusually Small Dust Grains in the Coma of Comet Hale–Bopp C/1995 O1', *Ap. J.* **549**, 635–646.

Matson, D. L.: 1972, '1. Astronomical Photometry at Wavelengths of 8.5, 10.5, and 11.6 μm. 2. Infrared Emission from Asteroids at Wavelengths 8.5, 10.5, and 11.6 μm', Ph.D. Thesis, California Institute of Technology.

McDonnell, J. A. M., Lamy, P. L., and Pankiewicz, G. S.: 1991, 'Physical Properties of Cometary Dust', in R. L. Newburn, Jr., M. Neugebauer, and J. Rahe (eds.), *Comets in the Post-Halley Era*, Kluwer Academic Publishers, Dordrecht.

McNaught, R. H.: 1995, 'Comet C/1995 O1 (Hale–Bopp)', *IAU Circ.* **6198**.

Meech, K. J., Buie, M. W., Samarasinha, N. H., Mueller, B. E. A., and Belton, M. J. S.: 1997, 'Observations of Structures in the Inner Coma of Chiron with the HST Planetary Camera', *A.J.* **113**, 844–862.

Millis, R. L., A'Hearn, M. F., and Campins, H.: 1988, 'An Investigation of the Nucleus and Coma of Comet P/Arend–Rigaux', *Ap. J.* **324**, 1194–1209.

Molina, A., and Moreno, F.: 1999, 'Comet Hale–Bopp as a Free-Rotation Rigid Body', *A. & A.* **347**, 366–369.

Morrison, D.: 1973, 'Determination of Radii of Satellites and Asteroids from Radiometry and Photometry', *Icarus* **19**, 1–14.

Müller, M., Green, S. F., and McBride, N.: 2002, 'An Easy-to-Use Model for the Optical Thickness and Ambient Illumination within Cometary Dust Comae', these proceedings.

Müller, T. G. and Lagerros, J. S. V.: 1998, 'Asteroids as Far-Infrared Photometric Standards for ISOPHOT', *A. & A.* **338**, 340–352.

Ostro, S. J.: 1982, 'Radar Properties of Europa, Ganymede, and Callisto', in D. Morrison (eds.), *Satellites of Jupiter*, University of Arizona Press, Tucson.

Prialnik, D.: 2002, 'Modeling the Comet Nucleus Interior. Application to Comet C/1995 O1 Hale–Bopp', these proceedings.

Qi, C.: 2000, 'Aperture Synthesis Studies of the Chemical Composition of Protoplanetary Disks and Comets', Ph.D. Thesis, Caltech.

Salo, H.: 1988, 'Monte Carlo Modeling of the Net Effects of Coma Scattering and Thermal Reradiation on the Energy Input to Cometary Nucleus [sic]', *Icarus* **76**, 253–269.

Samarasinha, N. H.: 2000, 'The Coma Morphology Due to an Extended Active Region and the Implications for the Spin State of Comet Hale–Bopp', *Ap. J.* **529**, L107–L110.

Samarasinha, N. H. and Belton, M. J. S.: 1995, 'Long-Term Evolution of Rotational Stress and Nongravitational Effects for Halley-Like Cometary Nuclei', *Icarus* **116**, 340–358.

Samarasinha, N. H., Mueller, B. E. A., and Belton, M. J. S.: 1997, 'Coma Morphology and Constraints on the Rotation of Comet Hale–Bopp (C/1995 O1)', *Earth Moon Planets* **77**, 189–198.

Sarmecanic, J., Fomenkova, M., Jones, B., and Lavezzi, T.: 1997, 'Constraints on the Nucleus and Dust Properties from Mid-Infrared Imaging of Comet Hyakutake', *Ap. J.* **483**, L69–L72.

Schleicher, D. G., Lederer, S. M., Millis, R. L., and Farnham, T. L.: 1997, 'Photometric Behavior of Comet Hale–Bopp (C/1995 O1) before Perihelion', *Science* **275**, 1913–1915.

Sekanina, Z.: 1988, 'Nucleus of Comet IRAS–Araki–Alcock (1983 VII)', *A.J.* **95**, 1876–1894.

Sekanina, Z.: 1997a, 'A Determination of the Nuclear Size of Comet Hale–Bopp (C/1995 O1)', *Earth Moon Planets* **77**, 147–153.

Sekanina, Z.: 1997b, 'Detection of a Satellite Orbiting the Nucleus of Comet Hale–Bopp (C/1995 O1)', *Earth Moon Planets* **77**, 155–163.

Sekanina, Z. and Boehnhardt, H.: 1997, 'Comet C/1995 O1 (Hale–Bopp)', *IAU Circ.* **6542**.

Soderblom, L. A., Becker, T. L., Bennett, G., Boice, D. C., Britt, D. T., Brown, R. H., Buratti, B. J., Isbell, C., Giese, B., Hare, T., Hicks, M. D., Howington-Kraus, E., Kirk, R. L., Lee, M., Nelson, R. M., Oberst, J., Owen, T. C., Rayman, M. D., Sandel, B. R., Stern, S. A., Thomas, N., and Yelle, R. V.: 2002, 'Observations of Comet 19P/Borrelly by the Miniature Integrated Camera and Spectrometer Aboard Deep Space 1', *Science* **296**, 1087–1091.

Vasundhara, R. and Chakraborty, P.: 1999, 'Modeling of Jets from Comet Hale–Bopp (C/1995 O1): Observations from the Vainu Bappu Observatory', *Icarus* **140**, 221–230.

Weaver, H. A. and Lamy, P. L.: 1997, 'Estimating the Size of Hale–Bopp's Nucleus', *Earth Moon Planets* **79**, 17–33.

Weaver, H. A., Feldman, P. D., A'Hearn, M. F., and Arpigny, C.: 1997, 'The Activity and Size of the Nucleus of Comet Hale–Bopp (C/1995 O1)', *Science* **275**, 1900–1904.

Weaver, H. A., Feldman, P. D., A'Hearn, M. F., Arpigny, C., Brandt, J. C., and Stern, S. A.: 1999, 'Post-Perihelion HST Observations of Comet Hale–Bopp (C/1995 O1)', *Icarus* **141**, 1–12.

Weissman, P. R. and Kieffer, H. H.: 1981, 'Thermal Modeling of Cometary Nuclei', *Icarus* **47**, 302–311.

Weissman, P. R. and Lowry, S. C.: 2001, 'The Size Distribution of Cometary Nuclei', *Bull. Amer. Astron. Soc.* **33**, 1094–1094.